Physicochemical Properties, Structure, and Conformations of 1-Butyl-3-methylimidazolium Bis(trifluoromethanesulfonyl)imide [C_4mim]NTf_2 Ionic Liquid

Andrey V. Blokhin, Yauheni U. Paulechka, Aliaksei A. Strechan, and Gennady J. Kabo*

Chemistry Faculty, Research Institute for Physical Chemical Problems, Belarusian State University, Leningradskaya 14, 220030 Minsk, Belarus

Received: November 14, 2007; In Final Form: January 10, 2008

Thermodynamic properties of 1-butyl-3-methylimidazolium bis(trifluoromethanesulfonyl)imide ([C_4mim]NTf_2) ionic liquid have been studied by adiabatic calorimetry in the temperature range of 5 to 370 K. This compound has been found to form crystal, liquid, and glass. The temperature and enthalpy of fusion for [C_4mim]NTf_2 have been determined to be $T_{fus} = 270.22 \pm 0.02$ K and $\Delta_{fus}H = 23.78 \pm 0.04$ kJ·mol^{-1}, respectively. The heat capacity of crystalline [C_4mim]NTf_2 in the T range of 205 to 255 K may vary by a few percent, subject to the procedure of the crystal preparation. The glass transition temperature for [C_4mim]NTf_2 has been found to be $T_g = 181.5 \pm 0.1$ K. On the basis of the results of DFT quantum chemical calculations, the experimental vibrational spectra, and the available literature data, thermodynamic properties of [C_4mim]NTf_2 in the ideal-gas state have been calculated by the statistical thermodynamic methods. The entropy values for the gaseous compound obtained from the experimental data and the calculations are in satisfactory agreement.

Introduction

Room-temperature ionic liquids (ILs) are considered to be a possible alternative to traditional solvents as components of reactive systems, heat carriers, electrolytes, and so forth.[1] Application of ILs in technology requires reliable values of their physicochemical properties including heat capacities, fusion temperatures, and enthalpies and entropies of phase transitions.

Earlier, the authors studied a series of 1-alkyl-3-methylimidazolium bis(trifluoromethanesulfonyl)imides ([$C_n$mim]NTf_2) by the adiabatic calorimetry.[2,3] It was found that [C_2mim]NTf_2 forms four crystalline modifications with various fusion temperatures, and [C_8mim]NTf_2 forms three sequences of crystalline phases with various T_{fus}. In addition, the heat capacity of some crystalline phases of [$C_n$mim]NTf_2 above $T = 200$ K depends on a procedure of obtaining the crystalline phase.[2] Additivity in the heat capacity and the entropy for these ILs was reported.[2]

The saturated vapor pressure was measured for [$C_n$mim]NTf_2 by the Knudsen method[4,5] and for [C_2mim]NTf_2 by the transpiration method.[6] The enthalpies of vaporization were calculated from the temperature dependence of the saturated vapor pressure. The vaporization enthalpies for these compounds were also determined in a drop calorimeter[7] and by the line-of-sight mass spectrometry.[8]

The values of thermodynamic properties obtained from experiment so far allow one to find the entropy of [$C_n$mim]NTf_2 in the gaseous state. Thermodynamic properties in the ideal-gas state can also be calculated by the statistical thermodynamic methods using molecular and spectral data.

In this work the results of heat capacity measurements in a range of temperatures of 5−370 K for 1-butyl-3-methylimidazolium bis(trifluoromethanesulfonyl)imide ([C_4mim]NTf_2) by adiabatic calorimetry are presented. The parameters of fusion and glass transition for this compound are reported. Thermodynamic properties of this compound in the ideal-gas state calculated by the statistical thermodynamic method are also presented.

Experimental Section

A sample of [C_4mim]NTf_2 was kindly provided by Prof. A. Heintz from the University of Rostock (Germany). The initial purity of the sample was >98% (mass fraction). [C_4mim]NTf_2 contained 28.14% C, 3.59% H, and 9.28% N as determined by the elemental analysis. The chloride ion was not discovered upon addition of $AgNO_3$. The sample was evacuated at $p < 1$ Pa and $T = 290$ K for 10 h. A mole fraction purity of the sample prepared in such a way was determined by the fractional melting technique in an adiabatic calorimeter to be 0.985.

The measurements of the condensed-state heat capacity in the temperature range of 5−370 K and the fusion enthalpy for [C_4mim]NTf_2 were conducted in a Termis TAU-10 adiabatic calorimeter.[9] The calorimeter design, the measurement procedure, and the results of measurements for reference compounds have been reported earlier.[3] The temperature was measured by the iron−rhodium resistance thermometer of $R_0 \sim 50$ Ohm calibrated on the ITS-90 scale at VNIIFTRI (Moscow). The maximum error of the measurements does not exceed $\pm 4 \times 10^{-3} C_p$ in the main measurement range of 20−370 K, $\pm 1 \times 10^{-2} C_p$ at $T = 10-20$ K, and $\pm 2 \times 10^{-2} C_p$ at $T < 10$ K. The [C_4mim]NTf_2 sample mass was 1.2250 g.

The infrared spectra of ILs in KBr pellets or in thin films were recorded at $T = 290$ K by a Brucker Vertex 70 spectrometer with a 1 cm^{-1} resolution and accumulation of 32 spectra.

The quantum chemical calculations were performed using the PC GAMESS 7.0 software.[10]

Results and Discussion

The experimental heat capacities for [C_4mim]NTf_2 in the temperature range of 5−370 K are presented in Table 1S (Supporting Information) and Figures 1 and 2. The detailed

* To whom correspondence should be addressed. Telephone: +375-17-2003916. Fax: +375-17-2003916. E-mail: kabo@bsu.by.

10.1021/jp710872s CCC: $40.75
Published on Web 03/15/2008

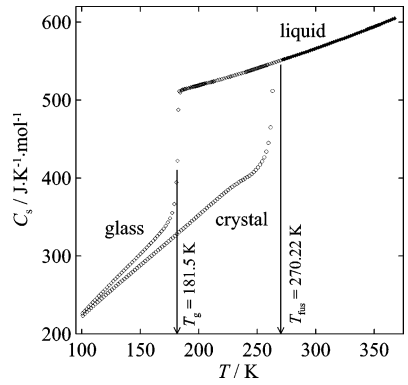

Figure 1. Experimental heat capacities of $[C_4mim]NTf_2$ between 100 and 370 K: ◇, glass and supercooled liquid (at $T < T_{fus}$); ◆, liquid (at $T > T_{fus}$); ○, crystal (series 2).

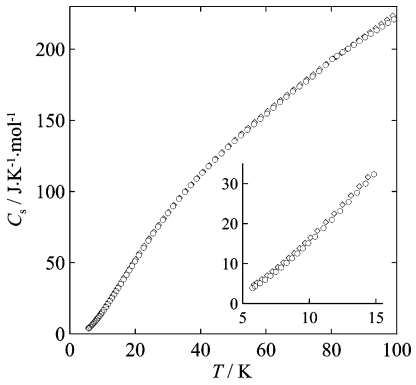

Figure 2. Experimental heat capacities of $[C_4mim]NTf_2$ at the vapor saturation pressure between 5 and 100 K: ◇, glass; ○, crystal (series 2 and 16).

description of the calorimetric measurements including series number, procedures for obtaining the phases, and temperature ranges of the measurements are given in Table 1.

Glass, Supercooled Liquid. Liquid $[C_4mim]NTf_2$ can supercool and form glass when cooled from $T = 300$ K at an initial rate of 20−30 mK·s^{-1}. The heat capacity of the glass was measured in series 1 and 17. Devitrification of the sample occurred in a range of $T = 170-186$ K.

The heat capacity of the supercooled liquid was measured from the temperatures just above the "glass → supercooled liquid" transition temperature to $T = 200$ K. Above the latter temperature, spontaneous crystallization of the sample occurred (series 1). At higher temperatures, the heat capacity of the supercooled liquid was measured in special experiments (series 9, 11−15). When cooled to $T = 194$ K, the liquid remained stable on the time scale of calorimetric measurements, as was observed in series 11−14. Only after the glass transition range was reached upon cooling to $T = 181$ K, crystallization of the supercooled phase occurred in the experiments at $T > 204$ K (series 15). This feature in the thermal behavior of supercooled $[C_4mim]NTf_2$ allowed us to measure its heat capacity over the entire temperature range from T_g to T_{fus}.

The temperature corresponding to the average heat capacity of the substance in the glass transition region was assumed to be a glass transition temperature $T_g = 181.5 \pm 0.1$ K. The T_g value was $0.672T_{fus}$, and this is in a good agreement with a well-known empirical rule, $T_g/T_{fus} = 2/3$.

The heat capacity jump at the glass transition $\Delta^l_{gl}C_{p,m} = 155 \pm 3$ J·K^{-1}·mol^{-1} is determined as a heat capacity difference between the liquid and the glass at T_g. The heat capacities of the glass $C_{p,m}$(gl, T_g) and the supercooled liquid $C_{p,m}$(sup.liq., T_g) were calculated from the equations

$$C_{p,m}(\text{gl})/\text{J·K}^{-1}\text{·mol}^{-1} = 258.3 - 0.8772(T/\text{K}) + 7.811 \times 10^{-3}(T/\text{K})^2 \quad (1)$$

$$C_{p,m}(\text{sup.liq.})/\text{J·K}^{-1}\text{·mol}^{-1} = 474.2 + 4.956 \times 10^{-2}(T/\text{K}) + 8.682 \times 10^{-4}(T/\text{K})^2 \quad (2)$$

obtained from the least-squares fit of the experimental heat capacities of the glass in the temperature range of 150−170 K and the supercooled liquid in a range of temperatures of 186−270 K.

The $\Delta^l_{gl}C_{p,m}$ value of $[C_4mim]NTf_2$ is not anomalous. $\Delta^l_{gl}C_{p,m}$ increases systematically in a line of $[C_nmim]NTf_2$: $\Delta^l_{gl}C_{p,m} = 155$ J·K^{-1}·mol^{-1} for $[C_4mim]NTf_2$, 171 J·K^{-1}·mol^{-1} for $[C_6mim]NTf_2$,[3] and 198 J·K^{-1}·mol^{-1} for $[C_8mim]NTf_2$.[2]

The residual entropy and the residual enthalpy of glassy $[C_4mim]NTf_2$

$$S^o_m(\text{gl}, T \rightarrow 0) = 19.3 \pm 3.9 \text{ J·K}^{-1}\text{·mol}^{-1}$$

$$H^o_m(\text{gl}, T \rightarrow 0) = 9.67 \pm 0.50 \text{ kJ·mol}^{-1}$$

were calculated from the equations

$$S^o_m(\text{gl}, T \rightarrow 0) = \frac{\Delta_{fus}H^o_m}{T_{fus}} - \int_0^{T_{fus}} \frac{C_{p,m}(\text{gl,liq}) - C_{p,m}(\text{cr})}{T'} dT' \quad (3)$$

$$H^o_m(\text{gl}, T \rightarrow 0) = \Delta_{fus}H^o_m - \int_0^{T_{fus}} [C_{p,m}(\text{gl,liq}) - C_{p,m}(\text{cr})]dT' \quad (4)$$

where $C_{p,m}$(cr) is heat capacity of the crystal and $\Delta_{fus}H^o_m$ is the fusion enthalpy. The relatively low $S^o_m(\text{gl}, T \rightarrow 0)$ value reveals a high degree of ordering in the structure of the glass. This fact is also confirmed by minute differences in heat capacities of the crystal and the glass at $T < 100$ K (Figure 2).

Existence of Metastable Crystal Phases. The heat capacity of crystalline $[C_4mim]NTf_2$ at $T > 205$ K significantly varies depending on a crystallization procedure (Figures 3 and 4). The crystal with the highest heat capacity in the temperature range of 205−255 K has the highest stability. The process of its formation from metastable crystals is accompanied by an exothermic effect.

On the basis of the preliminary experiments, the following procedure was applied to obtain the stable $[C_4mim]NTf_2$ crystal. After crystallization of the supercooled liquid, the calorimeter was heated to $T = 252$ K at a rate of 5 mK·s^{-1}. Then, the obtained crystal was annealed at $T = 252-253$ K for 6 h. An anomaly at $T > 210$ K with a weak maximum in the interval of 225−235 K was observed in the C_p versus T curve for this crystal (Figure 3, series 2).

In order to clarify the nature of this anomaly, the supercooled liquid was crystallized in such a way that the maximum temperature did not exceed $T = 230$ K. In series 3, during crystallization, the sample temperature was allowed to rise from $T = 202$ to 225 K. Then, the sample was heated to $T = 230$ K at a rate of 5 mK·s^{-1} and kept at this temperature for 18 h. The heat capacity of the crystals from series 2 and 3 agree within $1 \times 10^{-3}C_p$ in the range of 140−205 K (Figure 4), but at $T > 205$ K, the heat capacity of the crystal in series 3 is less than that in series 2 by $< 1.2 \times 10^{-2}C_p$. Moreover, the measurements

TABLE 1: Summary of Calorimetric Experiments for [C_4mim]NTf_2

	preparation procedure			heat capacity measurements	
series	1. formation	2. annealing	3. cooling	phases	temperature range
1	cooling of liquid		from 300 to 77 K	glass	80 K to T_g
				supercooled liquid	T_g to 200 K
				crystal	235 K to T_{fus}
				liquid	275−284 K
2	crystallization of supercooled liquid in the temperature range of 200−252 K	6 h at 252−253 K	to 78 K	crystal	80 K to T_{fus}
				liquid	T_{fus} to 276 K
3	crystallization of supercooled liquid in the temperature range of 200−230 K	18 h at 230 K	to 142 K at a rate of 0.02−0.01 K·s^{-1}	crystal[a]	143−254 K
4	cooling of crystal (after series 3)		from 255 to 199 K	crystal	200−248 K
5	annealing of crystal after series 4 for 3 h at 245 K, cooling at a rate of 2 mK·s^{-1} to 230 K	20 h at 230 K		crystal	231−235 K
6	cooling of crystal after series 5		from 236 K to 203 K	crystal	204 K to T_{fus}
7	crystallization of supercooled liquid in the temperature range of 200−225 K	1) 2 h at 225 K	1) from 225 to 216 at a rate of 5 mK·s^{-1}	crystal[a]	198−254 K
		2) 20 h at 216 K	2) from 216 to 197 at a rate of 10 mK·s^{-1}		
8	annealing of crystal (after series 7) for 2 h at 255 K and cooling		from 255 to 238 K	crystal	239 K to T_{fus}
9	cooling of liquid		from 300 to 240 K	supercooled liquid, liquid	241−354 K
10	cooling of liquid (after series 9)		from 355 to 343 K	liquid	344−368 K
11	cooling of liquid (after series 10)		from 370 to 224 K	supercooled liquid	225−258 K
12	cooling of supercooled liquid (after series 11)		from 259 to 210 K	supercooled liquid	211−227 K
13	cooling of supercooled liquid (after series 12)		from 228 to 204 K	supercooled liquid	205−213 K
14	cooling of supercooled liquid (after series 13)		from 214 to 194 K	supercooled liquid	195−205 K
15	cooling of supercooled liquid (after series 14)		from 206 to 181 K	supercooled liquid	182−204 K
16	like that in series 2	6 h at 252−253 K	to 77 K (nitrogen bath) and then to 5.5 K (helium bath)	crystal	5.7−84 K
17	like that in series 1		from 300 to 77 (nitrogen bath) and then to 5.5 K (helium bath)	glass	5.8−85 K

[a] Metastable phase.

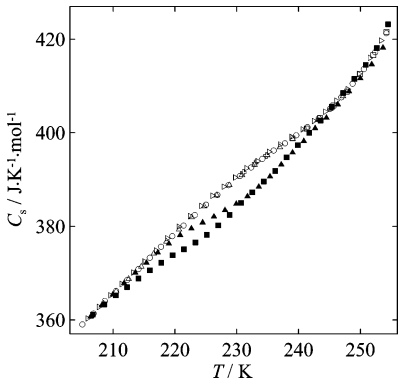

Figure 3. Heat capacities of crystalline [C_4mim]NTf_2 between 205 and 255 K. Stable crystals: ○, series 2; △, series 4; +, series 5; right-pointed triangle, series 6; □, series 8. Metastable crystals: ▲, series 3; ■, series 7.

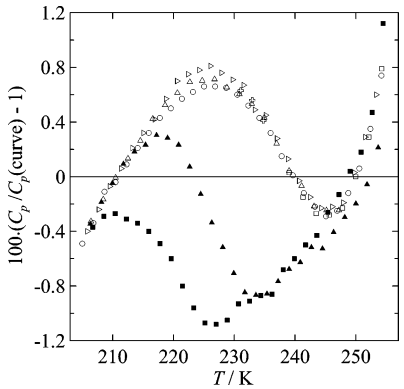

Figure 4. Relative deviation of the heat capacities of crystalline [C_4mim]NTf_2 in various series from the values C_p(curve)/J·K^{-1}·mol^{-1} = 302.7 − 0.4293(T/K) + 3.476 × 10^{-3}(T/K)^2: ○, series 2; ▲, series 3; △, series 4; +, series 5; right-pointed triangle, series 6; ■, series 7; □, series 8.

at T > 230 K in series 3 were accompanied by spontaneous heat evolution, as observed by high positive temperature drifts of the calorimeter in this temperature range (Figure 5). Immediately after the crystal reached T = 255 K, the sample was cooled to T = 199 K. After that, its heat capacity was measured in series 4. As a result, a heat capacity curve of the crystal from series 2 was reproduced (Figures 3 and 4), and the ordinary temperature drifts of the calorimeter were observed over the entire range of 200−248 K (Figure 5). Annealing the obtained crystal at T = 230 K for 20 h (series 5) and repeating

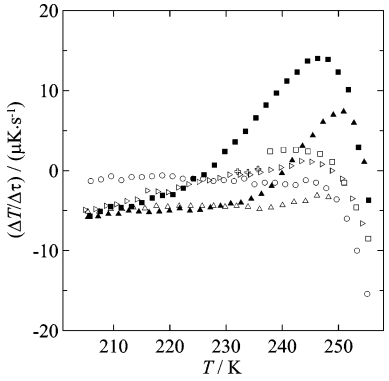

Figure 5. Temperature drifts during the heat capacity measurements of crystalline $[C_4mim]NTf_2$ in the temperature range of 200−255 K: ○, series 2; ▲, series 3; △, series 4; +, series 5; right-pointed triangle, series 6; ■, series 7; □, series 8.

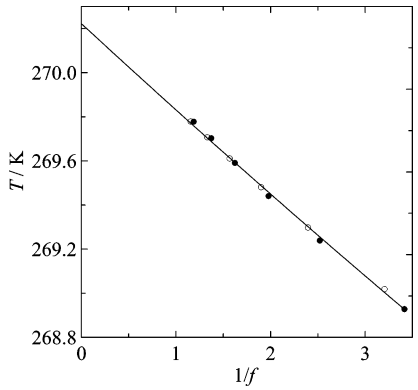

Figure 6. Results of the fractional melting experiments for $[C_4mim]NTf_2$: ○, series 6; ●, series 8.

measurements in the anomaly range (series 6) do not have a pronounced effect on the heat capacity values of the crystals in the temperature range of $T > 200$ K.

In series 7, after crystallization at $T = 225$ K and annealing at this temperature for 2 h, the calorimeter was slowly cooled to $T = 216$ K and kept at this temperature for 20 h. The heat capacities of the crystals from series 2, 3, and 7 agree within $1 \times 10^{-3} C_p$ near $T = 200$ K (Figure 4), while in the range of 210−230 K, the heat capacity of the crystal from series 7 is significantly lower than the values from series 2 and 3 (Figures 3 and 4). Spontaneous heat evolution accompanied the measurements for this crystal at $T > 220$ K (Figure 5). When the crystal reached $T = 255$ K and was annealed at this temperature for 2 h, the crystal similar to that in series 2 was obtained (series 8).

Earlier,[10,11] we found that the $[C_6mim]NTf_2$ metastable crystals obtained by crystallization of the supercooled liquid were stable in calorimetric measurements up to the premelting range. In the case of $[C_4mim]NTf_2$, they turned to be unstable when heated above their annealing temperatures. Differences in the heat capacity for the stable crystal obtained by different procedures (series 2, 4, 5, 6, 8) do not exceed $2 \times 10^{-3} C_p$ at $T > 200$ K (Figures 3 and 4) and are within the probable error of the calorimeter.

The exothermic effect of conversion of the metastable crystals into the stable form was less than -110 J·mol^{-1}, as estimated from the differences in temperature drifts of the calorimeter in the heat capacity measurements for these crystals (Figure 5). The enthalpy change over the range of 205−255 K for the stable crystal is higher than those for the unstable crystals. However, the differences do not exceed 125 J·mol^{-1}.

TABLE 2: The Results of Fractional Melting Experiments for $[C_4mim]NTf_2$

T/K	f	T/K	f
Series 1		Series 2	
269.019	0.3121	268.928	0.2928
269.298	0.4174	269.239	0.3969
269.481	0.5267	269.441	0.5055
269.611	0.6383	269.591	0.6163
269.707	0.7513	269.703	0.7285
269.779	0.8655	269.778	0.8423

TABLE 3: Determination of the Molar Enthalpy of Fusion for $[C_4mim]NTf_2$

series number or way of formation	T_{start}/K	T_{end}/K	Q/J·mol^{-1}	$\Delta_{fus}H_m^\circ$/J·mol^{-1}
series 6	243.56	272.31	36176	23746[a]
series 8	244.76	271.74	35417	23787[a]
like that in series 2	245.02	273.89	36515	23803[b]
like that in series 2	242.34	271.99	36524	23779[b]
			average	23779 ± 38

[a] From the fractional melting experiments. [b] From independent single-step experiments.

Fusion. The triple-point temperature $T_{fus} = 270.22 \pm 0.02$ K was determined from the fractional melting experiments (Figure 6, Table 2) with the use of the equation

$$\ln\left(\frac{\nu}{f} + 1\right) = \frac{\Delta_{fus}H_m^o}{RT_{fus}^2}\Delta T\left(1 + \left(\frac{1}{T_{fus}} - \frac{\Delta_{cr}^l C_p}{2\Delta_{fus}H_m^o}\right)\Delta T\right) \quad (5)$$

where $\Delta T = T_{fus} - T$; T is an equilibrium temperature corresponding to a melt fraction f, $\Delta_{fus}H_m^o$ is an enthalpy of fusion for a pure compound, $\Delta_{cr}^l C_p$ is a heat capacity jump at the fusion of a pure compound, and ν is an amount of impurities in a sample, mole per mole of the main substance.

The results of the fusion enthalpy determination for the stable crystal are presented in Table 3. Initial, T_{start}, and final, T_{end}, temperatures of the experiments lay outside of the temperature range of fusion. The fusion enthalpies were calculated from the equation

$$\Delta_{fus}H_m^o = Q - \int_{T_{start}}^{T_{fus}} C_{p,m}(cr)dT - \int_{T_{fus}}^{T_{end}} C_{p,m}(liq)dT \quad (6)$$

where Q is the energy spent to heat 1 mol of the compound from T_{start} to T_{end}. Heat capacities of the crystal and the liquid were approximated by the equations

$$C_{p,m}(cr)/J\cdot K^{-1}\cdot mol^{-1} = 1331.7 - 8.726(T/K) + 2.018 \times 10^{-2}(T/K)^2 \quad (7)$$

$$C_{p,m}(liq)/J\cdot K^{-1}\cdot mol^{-1} = 467.2 + 0.1301(T/K) + 6.646 \times 10^{-4}(T/K)^2 \quad (8)$$

obtained by the least-squares fit of the experimental heat capacities in the temperature range of 234−246 K for the crystal and 260−368 K for the liquid.

Standard Thermodynamic Functions. The smoothed heat capacities and the derived standard thermodynamic functions for $[C_4mim]NTf_2$ in the condensed state are presented in Table 4. The empirical equation

$$C_p = D_3(\theta_D) + 3E(\theta_E) \quad (9)$$

TABLE 4: Molar Thermodynamic Functions of [C4mim]NTf2 in the Condensed State (R = 8.314472 J·K^{-1}·mol^{-1})

T/K	$C_{p,m}/R$	$\Delta_0^T H_m^o/RT$	$\Delta_0^T S_m^o/R$	Φ_m^o/R^b	T/K	$C_{p,m}/R$	$\Delta_0^T S_m^o/RT$	$\Delta_0^T S_m^o/R$	Φ_m^o/R^b
		glass					crystal		
5	0.3745	0.09605	0.1285	0.03241	5	0.3156	0.07914	0.1055	0.02640
10	1.950	0.5927	0.8212	0.2286	10	1.846	0.5406	0.7394	0.1988
15	4.073	1.392	2.005	0.6128	15	3.957	1.320	1.877	0.5577
20	6.267	2.338	3.478	1.141	20	6.165	2.255	3.319	1.063
25	8.349	3.335	5.104	1.769	25	8.277	3.252	4.925	1.673
30	10.24	4.330	6.796	2.465	30	10.21	4.253	6.607	2.355
35	11.95	5.300	8.506	3.206	35	11.94	5.231	8.315	3.084
40	13.49	6.228	10.20	3.975	40	13.47	6.167	10.01	3.844
45	14.92	7.115	11.88	4.760	45	14.89	7.058	11.68	4.622
50	16.26	7.963	13.52	5.554	50	16.19	7.908	13.32	5.410
60	18.71	9.553	16.70	7.148	60	18.58	9.488	16.48	6.994
70	20.98	11.03	19.76	8.733	70	20.86	10.95	19.52	8.568
80	23.12	12.40	22.70	10.30	80	23.13	12.33	22.45	10.12
90	25.12	13.71	25.54	11.83	90	24.96	13.64	25.29	11.65
100	27.13	14.95	28.29	13.34	100	26.73	14.86	28.01	13.15
110	29.06	16.14	30.97	14.82	110	28.40	16.01	30.64	14.62
120	30.93	17.30	33.58	16.28	120	30.00	17.11	33.18	16.06
130	32.76	18.42	36.13	17.71	130	31.56	18.16	35.64	17.47
140	34.56	19.51	38.62	19.11	140	33.10	19.18	38.03	18.86
150	36.36	20.57	41.07	20.49	150	34.63	20.16	40.37	20.21
160	38.24	21.62	43.47	21.86	160	36.16	21.11	42.65	21.54
170	40.29	22.65	45.85	23.20	170	37.69	22.04	44.89	22.85
180	45.43	23.73	48.25	24.52	180	39.24	22.95	47.09	24.14
181.5	50.81	23.92	48.64	24.72	190	40.80	23.85	49.25	25.40
		supercooled liquid			200	42.39	24.74	51.39	26.65
190	61.94	25.56	51.42	25.85	210	43.98	25.62	53.49	27.88
200	62.40	27.40	54.60	27.21	220	45.54	26.49	55.57	29.09
210	62.89	29.07	57.66	28.59	230	46.96	27.35	57.63	30.29
220	63.40	30.62	60.60	29.98	240	48.09	28.19	59.65	31.47
230	63.93	32.06	63.43	31.37	250	(49.49)[a]	29.01	61.64	32.63
240	64.48	33.40	66.16	32.76	260	(51.37)[a]	29.83	63.62	33.79
250	65.05	34.65	68.80	34.15	270	(53.74)[a]	30.67	65.60	34.93
260	65.64	35.83	71.37	35.53	270.22	(53.80)[a]	30.69	65.65	34.95
270	66.24	36.95	73.86	36.91			liquid		
270.22	66.26	36.97	73.91	36.94	270.22	66.26	41.27	76.23	34.95
					280	66.84	42.16	78.60	36.44
					290	67.45	43.02	80.95	37.93
					298.15	67.96	43.69	82.83	39.13
					300	68.08	43.84	83.25	39.40
					310	68.72	44.64	85.49	40.86
					320	69.38	45.40	87.68	42.28
					330	70.06	46.14	89.83	43.69
					340	70.75	46.85	91.93	45.08
					350	71.46	47.54	93.99	46.45
					360	72.18	48.22	96.01	47.80
					370	(72.92)[a]	48.87	98.00	49.13

[a] Extrapolated values. [b] Φ_m^o is $\Phi_m^o = -(G_m^o(T) - H_m^o(0))/T = \Delta_0^T S_m^o - (\Delta_0^T H_m^o/T)$.

was used for heat capacity extrapolation to $T < 6$ K. Here, D is a Debye heat capacity function for three degrees of freedom, E is an Einstein heat capacity function for one degree of freedom, and θ_D and θ_E are the corresponding characteristic temperatures. The characteristic temperatures $\theta_D = 45.2$ K and $\theta_E = 49.5$ K for the crystal and $\theta_D = 42.1$ K and $\theta_E = 51.0$ K for the glass were obtained by the least-squares fit of the experimental heat capacities in the temperature ranges of 5.7−9.5 and 5.8−9.3 K, respectively. In these temperature ranges, the rms deviation between the experimental heat capacities and those calculated from eq 9 were $<1 \times 10^{-2} C_p$.

The standard thermodynamic properties of liquid [C4mim]NTf2 at $T = 298.15$ K are equal to

$$C_{p,m} = 565.1 \pm 2.3 \text{ J·K}^{-1}\text{·mol}^{-1}$$

$$\Delta_0^T S_m^o = 688.7 \pm 3.0 \text{ J·K}^{-1}\text{·mol}^{-1}$$

$$\Delta_0^T H_m^o/T = 363.3 \pm 1.6 \text{ J·K}^{-1}\text{·mol}^{-1}$$

$$\Phi_m^o = 325.4 \pm 3.4 \text{ J·K}^{-1}\text{·mol}^{-1}$$

Calculations

Ideal-Gas Thermodynamic Properties. In the calculation of properties for gaseous [C4mim]NTf2, it is assumed that the vapor consists of ionic pairs. The molar mass of the ionic pair is 0.4194 kg·mol^{-1}.

On the basis of the results of quantum chemical calculations for the 1-alkyl-3-methylimidazolium ionic pairs with various cations,[12,13,14] it is expected that in the most stable configuration of the ionic pair, the anion is positioned near the C(2) atom of the cation. The configuration demonstrated in Figure 7 was accepted as a base configuration for the statistical thermodynamic calculations. Its geometry was optimized at the B3LYP/6-31+G(d) level. The product of the principal moments of inertia is $I_A I_B I_C = 1.674 \times 10^{-130}$ kg^3·m^6, and the symmetry number is $\sigma = 1$.

The number of normal modes of the [C4mim]NTf2 ionic pair is $3 \times 40 - 6 = 114$. Corresponding frequencies were calculated by the B3LYP/6-31+G(d) method. To determine scaling factors for the ionic pair frequencies, the assignment of frequencies in the vibrational spectra of the cation and the anion was performed

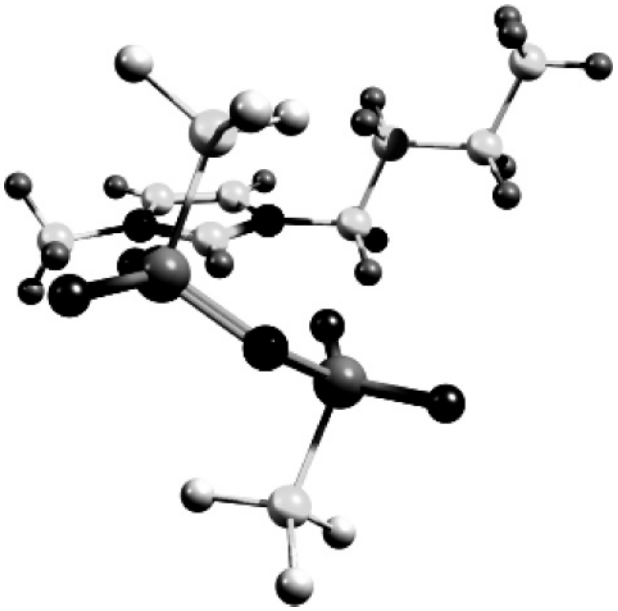

Figure 7. Configuration of a $[C_4mim]NTf_2$ ionic pair.

based on the experimental IR spectra of NTf_2^-- and $[C_4mim]^+$-containing ILs and the results of quantum chemical calculations at the mentioned theory level (Figure 8). The experimental vibrational spectra for ILs[15−19] were also used. The equations for the scaling factors were found to be for the cation

$$\upsilon_{exp} = 0.945\upsilon_{calc} \text{ above } 1700 \text{ cm}^{-1}$$

$$\upsilon_{exp} = \upsilon_{calc}(1.022 - 3.30 \times 10^{-5}\upsilon_{calc}) \text{ below } 1700 \text{ cm}^{-1}$$

and those for the anion are

$$\upsilon_{exp} = \upsilon_{calc}(1.161 - 2.46 \times 10^{-4}\upsilon_{calc}) \text{ above } 500 \text{ cm}^{-1}$$

$$\upsilon_{exp} = \upsilon_{calc}(1.065 - 3.08 \times 10^{-4}\upsilon_{calc}) \text{ below } 500 \text{ cm}^{-1}$$

The ionic pair frequencies with a major contribution from intramolecular vibrations of the cation were scaled by the cation's scaling factors, and those caused by the anion vibrations were scaled by the anion's scaling factors. Frequencies of the cation−anion vibrations were scaled by the anion's scaling factors.

The following set of frequencies (in cm^{-1}) was applied in the calculations:

[10.3], 13.8, [23.5], 32.4, [36.5], [43.5], 50.0, 57.1, 70.8, 76.8, 100, 108, 116, 126, [135], 135, 200, 205, 213, 218, 233, [245], 252, 284, 303, 303, 317, 321, 330, 348, 350, 401, 415, 425, 436, 510, 541, 558, 567, 576, 590, 609, 629, 630, 635, 667, 735, 737, 741, 748, 775, 790, 808, 841, 910, 933, 949, 1007, 1026, 1032, 1040, 1050, 1100, 1109, 1111, 1118, 1120, 1142, 1150, 1171, 1200, 1208, 1209, 1226, 1228, 1240, 1244, 1281, 1285, 1303, 1310, 1318, 1328, 1329, 1367, 1380, 1394, 1402, 1421, 1440, 1469, 1472, 1480, 1480, 1481, 1486, 1490, 1549, 1562, 2859, 2864, 2874, 2897, 2912, 2912, 2923, 2936, 2944, 2985, 2990, 3018, 3048, 3116, 3133

The anion forms two chiral conformers, cis and trans. The value $\Delta H(\text{trans}-\text{cis}) = 3.5 \pm 0.1$ kJ·mol^{-1} at $<T> = 348$ K was found from the temperature dependence of the $[C_2mim]NTf_2$ Raman spectrum in a liquid phase in the wavenumber range of 380−440 cm^{-1}.[16] This value was used in the present paper. The barrier to internal rotation of the C_{3-} top was calculated to be $V = 8.7$ kJ·mol^{-1}. The symmetry number of the top is $n_r = 3$, and the reduced moment of inertia is found, as described in ref 20, to be $I_r = 1.46 \times 10^{-45}$ kg·m^2. Contributions of internal rotation of the C_{3-} tops were calculated from the energy levels of a hindered rotor. The corresponding frequencies of 36.5 and 43.5 cm^{-1} marked by square brackets were excluded from the set.

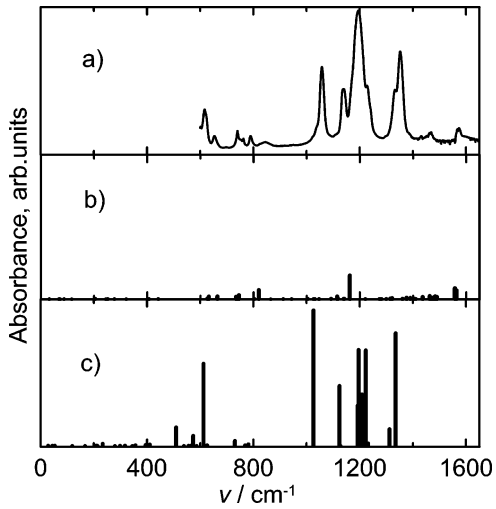

Figure 8. Experimental and calculated IR spectra; a) liquid $[C_4mim]NTf_2$, b) calculated spectrum for the tt conformer of $[C_4mim]^+$, and c) calculated spectrum for the trans conformer of NTf_2^-.

According to the ab initio calculations,[13] $[C_4mim]^+$ forms nine stable conformers, distinguishable in energy (Figure 9). Numbering of the conformers follows ref 13. Each conformer has a chiral pair. The C_s conformer of the cation was reported to be a flat maximum in a potential energy curve for the butyl top rotation. In this work, the energy differences between the conformers were determined from the B3LYP/6-31+G(d) calculations for the isolated cation (Figure 9, Table 5). The barriers to internal rotation of the Bu top were calculated to be 3.0 kJ·mol^{-1} (butyl group turned to the C(2) atom) and 6.0 kJ·mol^{-1} (butyl group turned from the C(2) atom). The potential energy curve for internal rotation of the Bu top was approximated by the equation

$$V(\varphi)/\text{kJ·mol}^{-1} = 2.31 + 1.50\cos\varphi + 2.19\cos 2\varphi \quad (10)$$

where φ is a phase angle. The reduced moment of inertia for this top is 2.40×10^{-45} kg·m^2, and the symmetry number is 1. The corresponding frequency 23.5 cm^{-1} was excluded from the complete set.

The barriers to internal rotation of the CH_3-(C) and CH_3-(N) tops were calculated to be 12.0 and 1.9 kJ·mol^{-1}. The reduced moments of inertia of the tops are equal to 5.24×10^{-47} and 5.34×10^{-47} kg·m^2, respectively. The symmetry number of the tops is 3. The frequencies of the corresponding torsional vibrations of 245 and 135 cm^{-1} were excluded from the complete set.

The possible configurations of the ionic pair were analyzed at the B3LYP/3-21+G(d) level. It was found that for a certain conformation of the cation, the configurations of the ionic pair can be divided into several groups (Figure 10): (a) NTf_2 placed "from" and "to" the cycle (2 variants); configurations a and b in Figure 10; (b) structures with different chiral conformers of NTf_2 (2); configurations a and c; and (c) NTf_2 staying below

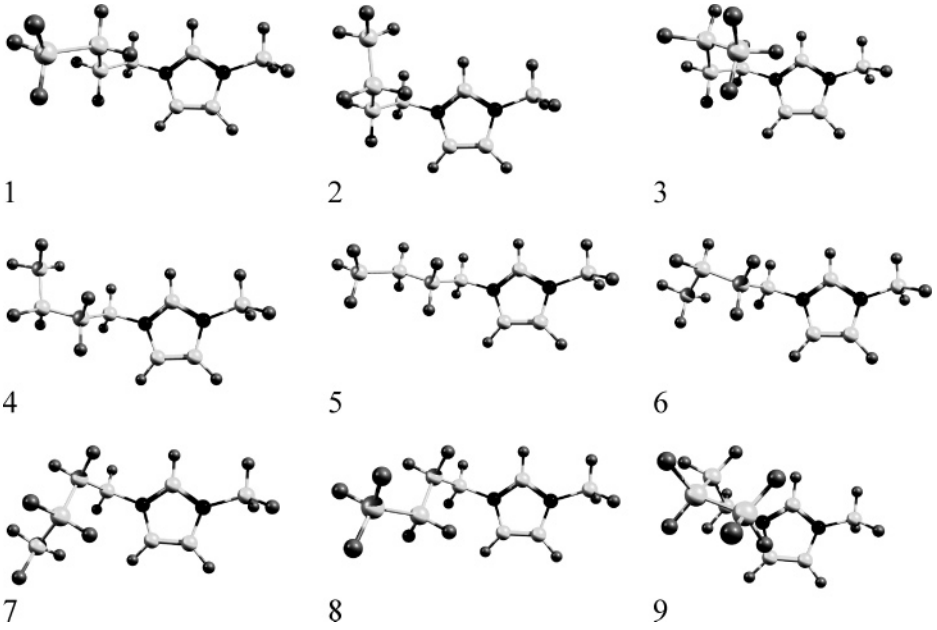

Figure 9. $[C_4mim]^+$ conformers.

TABLE 5: Relative Energies of the $[C_4mim]^+$ Conformers at $T = 0$ K

no.	ΔH_0/kJ·mol^{-1}	no.	ΔH_0/kJ·mol^{-1}
1	1.5	6	3.6
2	5.3	7	7.0
3	11.1	8	3.4
4	3.5	9	13.1
5	0.0		

and above the cycle (9); configurations schematically presented in Figure 10d.

The energy differences between the configurations do not exceed a few kJ·mol^{-1}. In the calculation of thermodynamic properties, it is assumed that all of the configurations are of the same energy.

Rotation of the NTf_2 top around the N(anion)−C(2) axis was assumed to be free, with the reduced moment of inertia of 1.11×10^{-44} kg·m^2 and the symmetry number of 2. The frequency of the corresponding torsional vibration 10.3 cm^{-1} was excluded from the complete set.

Thermodynamic properties of $[C_4mim]NTf_2$ in the ideal-gas state are presented in Table 6. The entropy of the gaseous $[C_4mim]NTf_2$, $S^o_{g,exp} = 1096$ J·K^{-1}·mol^{-1} at $T = 470$ K, was found from the experimental data according to the equation

$$S^o_{g,exp} = S^o_{liq} + \Delta_{vap}H^o/T + R\ln(p_{sat}/p^\circ) \qquad (11)$$

where $S^o_{liq} = 967$ J·K^{-1}·mol^{-1} is the entropy of the liquid, $\Delta_{vap}H^o = 119$ kJ·mol^{-1},[5] and $p_{sat} = 31$ mPa.[5] The liquid entropy

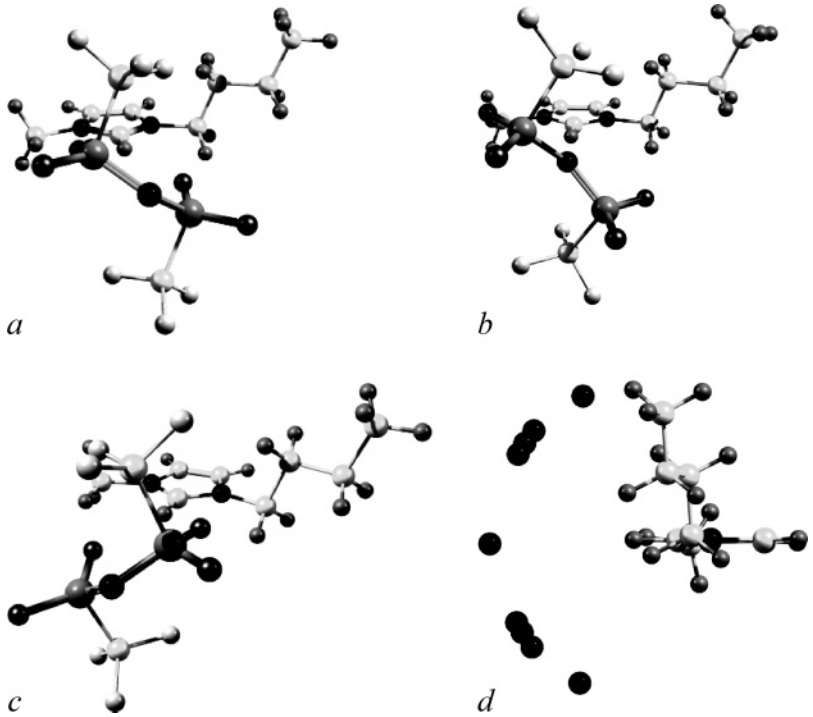

Figure 10. $[C_4mim]NTf_2$ ionic pair configurations; a−c are configurations with the anion nitrogen atom close to the imidazolium plane; d is a schematic representation of configurations with the anion below and above the ring; only the anion nitrogen atoms are shown.

TABLE 6: Molar Thermodynamic Functions of $[C_4mim]NTf_2$ in the Ideal-Gas State

T K	$C_{p,m}$ $J\cdot K^{-1}\cdot mol^{-1}$	$\Delta_0^T H_m^o/T$	S_m^o	Φ_m^o
100	208.3	131.2	551.3	420.1
200	316.5	198.2	730.8	532.6
298.15	407.4	252.2	874.3	622.0
400	493.8	303.0	1006	703.4
500	565.6	348.6	1125	775.9
600	623.8	389.8	1233	843.2
700	671.0	426.7	1333	906.1
800	709.5	459.7	1425	965.3
900	741.4	489.3	1510	1021
1000	768.0	515.9	1590	1074

at $T = 370$ K was found from the adiabatic calorimetric measurements, and the entropy change from $T = 370$ to 470 K was calculated using eq 8.

The $S^o_{g,exp}$ value is 6 $J\cdot K^{-1}\cdot mol^{-1}$ (0.6%) higher than the theoretical value $S^o_{calc}(470\ K) = 1090\ J\cdot K^{-1}\cdot mol^{-1}$. If one uses the vaporization enthalpy from ref 7, the value $S^o_{exp}(470\ K) = 1139\ J\cdot K^{-1}\cdot mol^{-1}$ is obtained, which is in worse agreement with the theoretical value; the difference is $\sim 4\%$.

Acknowledgment. The authors are grateful to Prof. A. Heintz for the provided sample of $[C_4mim]NTf_2$. This work was supported by the INTAS-Belarus foundation (Grant No. 03-50-5526).

Note Added in Proof. In a recent paper by Shimizu et al.,[21] the results of adiabatic measurements for $[C_4mim]NTf_2$ were presented. The reported heat capacities of liquid and the fusion enthalpy are in excellent agreement with those in the present paper and in ref 11.

Supporting Information Available: Experimental molar heat capacities of $[C_4mim]NTf_2$ in the condensed state at the vapor saturation pressure. This information is available free of charge via the Internet at http://pubs.acs.org.

References and Notes

(1) Wasserscheid, P., Welton, T., Eds. *Ionic Liquids in Synthesis*; Wiley: New York, 2002, 364 p.

(2) Paulechka, Y. U.; Blokhin, A. V.; Kabo, G. J.; Strechan, A. A. *J. Chem. Thermodyn.* **2007**, *39*, 866−877.

(3) Blokhin, A. V.; Kabo, G. J.; Paulechka, Y. U. *J. Chem. Eng. Data* **2006**, *51*, 1377−1388.

(4) Paulechka, Y. U.; Zaitsau, Dz. H.; Kabo, G. J.; Strechan, A. A. *Thermochim. Acta* **2005**, *439*, 158−160.

(5) Zaitsau, Dz. H.; Kabo, G. J.; Strechan, A. A.; Paulechka, Y. U.; Tschersich, A.; Verevkin, S. P.; Heintz, A. *J. Phys. Chem. A* **2006**, *110*, 7303−7306.

(6) Emel'yanenko, V. N.; Verevkin, S. P.; Heintz, A. *J. Am. Chem. Soc.* **2007**, *129*, 3930−3937.

(7) Santos, L. M. N. B. F.; Canongia Lopes, J. N.; Coutinho, J. A. P.; Esperanca, J. M. S. S.; Gomes, L. R.; Marrucho, I. M.; Rebelo, L. P. N. *J. Am. Chem. Soc.* **2007**, *129*, 284−285.

(8) Armstrong, J. P.; Hurst, C.; Jones, R. G.; Licence, P.; Lovelock, K. R. J.; Satterley, C. J.; Villar-Garcia, I. J. *Phys. Chem. Chem. Phys.* **2007**, *9*, 982−990.

(9) Pavese, F.; Malyshev, V. M. *Adv. Cryog. Eng.* **1994**, *40*, 119−124.

(10) Nemukhin, A. V.; Grigorenko, B. L.; Granovsky, A. A. *Moscow Univ. Chem. Bull.* **2004**, *45*, 75−102.

(11) Blokhin, A. V.; Paulechka, Y. U.; Kabo, G. J. *Thermochim. Acta* **2006**, *445*, 75−77.

(12) Paulechka, Y. U.; Kabo, G. J.; Blokhin, A. V.; Vydrov, O. A.; Magee, J. W.; Frenkel, M. *J. Chem. Eng. Data* **2003**, *48*, 457−462.

(13) Turner, E. A.; Pye, C. C.; Singer, R. D. *J. Phys. Chem. A* **2003**, *107*, 2277−2288.

(14) Katsuba, S. A.; Zvereva, E. E.; Vidiš, A.; Dyson, P. J. *J. Phys. Chem. A* **2007**, *111*, 352−370.

(15) Hayashi, S.; Ozawa, R.; Hamaguchi, H. *Chem. Lett.* **2003**, *32*, 498−499.

(16) Fujii, K.; Fujimori, T.; Takamuku, T.; Kanzaki, R.; Umebayashi, Y.; Ishiguro, S. *J. Phys. Chem. B* **2006**, *110*, 8179−8183.

(17) Umebayashi, Y.; Fujimori, T.; Sukizaki, T.; Asada, M.; Fujii, K.; Kanzaki, R.; Ishiguro, S. *J. Phys. Chem. A* **2005**, *109*, 8976−8982.

(18) Rajian, J. R.; Li, S.; Bartsch, R. A.; Quitevis, E. L. *Chem. Phys. Lett.* **2004**, *393*, 372−377.

(19) Castriota, M.; Caruso, T.; Agostino, R. G.; Cazzanelli, E.; Henderson, W. A.; Passerini, S. *J. Phys. Chem. A* **2005**, *109*, 92−96.

(20) Pitzer, K. S. *J. Chem. Phys.* **1946**, *14*, 239−243.

(21) Shimizu, Y.; Ohte, Y.; Yamamura, Y.; Saito, K. *Chem. Lett.* **2007**, *36*, 1484−1485.